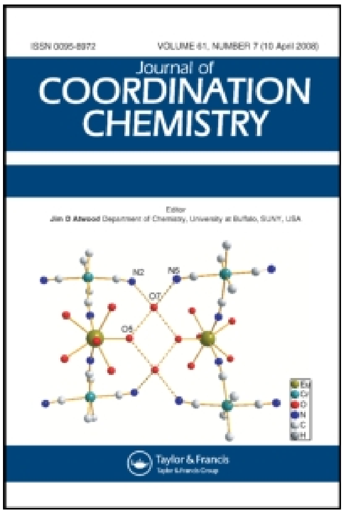

Journal of Coordination Chemistry
Publication details, including instructions for authors and subscription information:
http://www.informaworld.com/smpp/title~content=t713455674

Acetato and formato copper(II) paddle-wheel complexes with nitrogen ligands

Montserrat Barquín[a]; Nerea Cocera[a]; María J. González Garmendia[a]; Liher Larrínaga[a]; Elena Pinilla[bc]; María R. Torres[b]
[a] Grupo de Química Inorgánica, Facultad de Ciencias Químicas, Universidad del País Vasco, UPV/EHU, Apartado 1072, 20080 San Sebastián, Spain [b] Laboratorio de Difracción de rayos X, Facultad de Ciencias Químicas, Universidad Complutense, 28040 Madrid, Spain [c] Departamento de Química Inorgánica, Facultad de Ciencias Químicas, Universidad Complutense, 28040 Madrid, Spain

To cite this Article Barquín, Montserrat , Cocera, Nerea , González Garmendia, María J. , Larrínaga, Liher , Pinilla, Elena and Torres, María R.(2010) 'Acetato and formato copper(II) paddle-wheel complexes with nitrogen ligands', Journal of Coordination Chemistry, 63: 13, 2247 — 2260, First published on: 16 July 2010 (iFirst)

To link to this Article: DOI: 10.1080/00958972.2010.502227

URL: http://dx.doi.org/10.1080/00958972.2010.502227

Journal of Coordination Chemistry
Vol. 63, No. 13, 10 July 2010, 2247–2260

Taylor & Francis
Taylor & Francis Group

Acetato and formato copper(II) paddle-wheel complexes with nitrogen ligands

MONTSERRAT BARQUÍN*†, NEREA COCERA†,
MARÍA J. GONZÁLEZ GARMENDIA†, LIHER LARRÍNAGA†,
ELENA PINILLA‡§ and MARÍA R. TORRES‡

†Grupo de Química Inorgánica, Facultad de Ciencias Químicas, Universidad del País Vasco, UPV/EHU, Apartado 1072, 20080 San Sebastián, Spain
‡Laboratorio de Difracción de rayos X, Facultad de Ciencias Químicas, Universidad Complutense, 28040 Madrid, Spain
§Departamento de Química Inorgánica, Facultad de Ciencias Químicas, Universidad Complutense, 28040 Madrid, Spain

(*Received 11 January 2010; in final form 29 April 2010*)

Compounds $Cu(AcO)_2(pydz)$ (**1**), $Cu(HCOO)_2(pymd)_{1/2}$ (**2**), $Cu(AcO)_2(pymd)_{1/2}$ (**3**), and $Cu(AcO)_2(4,4'\text{-bipy})_{1/2}$ (**4**) were obtained by reactions of $Cu(AcO)_2{\cdot}H_2O$ and $Cu(HCOO)_2 \cdot 4H_2O$ with pyridazine, pyrimidine, or 4,4′-bipyridine. In all the studied structures, the *paddle-wheel* units $[Cu_2[\mu\text{-}RCOO)_4]$ are present. Coppers show a square pyramidal coordination determined by four oxygens in the equatorial positions and a nitrogen in the axial position. Compound **1** consists of centrosymmetric dimeric molecules. Compounds **2** and **3** instead consist of *zig-zag* chains of $[Cu_2[\mu\text{-}RCOO)_4]$ units linked by bridging pyrimidine molecules. The chains run in the (1 0 1) and (1 1 −2) directions in **2** and **3**, respectively. By crystallization of a solution of **4** in chloroform, $Cu(AcO)_2(4,4'\text{-bipy})_{1/2} \cdot 1/2CHCl_3$ (**5**) was obtained. It consists of monodimensional chains of $[Cu_2(\mu\text{-}CH_3COO)_4]$ units linked by bridging 4,4′-bipy molecules. The chains, of two different types, run parallel to the *b*-axis in the crystal. Two chlorines of each $CHCl_3$ molecule are close to two oxygens of two parallel chains. The packing can be described as sheets parallel to the (1 0 −1) plane. Magnetic properties and electron paramagnetic resonance spectra have been studied.

Keywords: Copper(II); Pyridazine; Pyrimidine; 4,4′-Bipyridine; Paddle-wheel complexes

1. Introduction

Dinuclear copper acetate dihydrate $[Cu_2(\mu\text{-}AcO)_4(H_2O)_2]$ and the adducts $[Cu_2(\mu\text{-}AcO)_4L_2]$ with different ligands in the axial positions are among the most studied dinuclear compounds of Cu(II) in their structural and magnetic aspects [1–6]. On the contrary, few compounds containing the *paddle-wheel* dinuclear group $[Cu_2(\mu\text{-}HCOO)_4]$, with four *syn–syn* formate groups, are known. This structure is present in some complexes: molecular dimers as $[Cu_2(\mu\text{-}HCOO)_4(urea)_2]$ [7], $[Cu_2(\mu\text{-}HCOO)_4(dmso)_2]$ [8], and $[Cu_2(\mu\text{-}HCOO)_4(dmf)_2]$ [9], chains of dimers

---

*Corresponding author. Email: montserrat.barquin@ehu.es

Journal of Coordination Chemistry
ISSN 0095-8972 print/ISSN 1029-0389 online © 2010 Taylor & Francis
DOI: 10.1080/00958972.2010.502227

as $\cdots$ dioxane–[$Cu_2(\mu\text{-}HCOO)_4$]–dioxane–[$Cu_2(\mu\text{-}HCOO)_4$] $\cdots$ [10], and dimers or chains of dimers with pyrazine and different isomers of dimethylpyrazine [11].

The copper(II) formate tetrahydrate, $Cu(HCOO)_2{\cdot}4H_2O$, does not have the dinuclear unit [$Cu_2(\mu\text{-}HCOO)_4$], similar to that of copper(II) acetate. It consists of chains $\cdots$–$Cu(H_2O)_2$–(μ-HCOO)$_2$–$Cu(H_2O)_2$–(μ-HCOO)$_2$–$\cdots$, with *anti–anti* bridging $HCOO^-$, linked by hydrogen bonds through additional water molecules [12].

In previous articles, we reported the complexes with 2-(phenylamino)pyridine and 2-(methylamino)pyridine, [$Cu_2(\mu\text{-}AcO)_4(PhNHpy)_2$] [13], [$Cu_2(\mu\text{-}AcO)_4(MeNHpy)_2$] [14] and [$Cu_2(\mu\text{-}HCOO)_4(PhNHpy)_2$], and [$Cu_2(\mu\text{-}HCOO)_4(MeNHpy)_2$] [15]. All these compounds are molecular dimers with the *paddle-wheel* unit [$Cu_2(\mu\text{-}RCOO)_4$] and nitrogen ligands coordinated in the axial positions.

Compounds containing the dimeric *paddle-wheel* copper(II) units with diverse carboxylate and dicarboxylate groups receive much attention [16, 17].

Pyridazine (pydz) is a ligand with two nitrogens in 1,2 positions. A few compounds have been described with pydz as bridging ligand. This is the case of [$\{Cu(pydz)\}_4(\gamma\text{-}H_4Mo_8O_{26})$] with {$Cu_2(pydz)_2$} units [18] and $Cu(pydz)Cl_2$, *zig-zag* chains of $CuCl_2$ units linked by pydz molecules [19]. Pyrimidine (pymd), on the other hand, has two nitrogens in 1,3 positions, and it can adopt bridging coordination as in the 1-D coordination polymers, $[M(NO_3)_2(pymd)(H_2O)_2]_\infty$ [M = Mn, Co, Ni, and Zn] [20]. Monodentate and bridging coordination of pymd in polymers of Cu(II)–dicyanamide–pyrimidine have been described [21].

4,4′-Bipyridine (4,4′-bipy) is a rigid spacer very often employed in the construction of coordination frameworks. An example is $Cu(HCOO)_2$(4,4′-bipy) polymer, with a 3-D structure, in which the coppers are connected through four formate anions and two 4,4′-bipy bridging molecules [22]. Other complexes of $Cu_2(AcO)_4$(4,4′-bipy)$\cdot$S (S = DMF and CH_3CN) composition have been described [23–25]. In all these cases the structure consists of 1-D chains of *paddle-wheel* units and 4,4′-bipy molecules, but the global structure changes depending on the solvent.

In this article, we describe the molecular dimer [$Cu_2(\mu\text{-}AcO)_4(pydz)_2$] (**1**) and the polymer chains $\{[Cu_2(\mu\text{-}HCOO)_4](\mu\text{-}pymd)\}_n$ (**2**) and $\{[Cu_2(\mu\text{-}AcO)_4](\mu\text{-}pymd)\}_n$ (**3**), formed by [$Cu_2(\mu\text{-}RCOO)_4$] groups linked by a bridging pymd, with the purpose of verifying the different coordination modes of pydz and pymd. We also report the formation of $\{[Cu_2(\mu\text{-}AcO)_4](\mu\text{-}4,4'\text{-}bipy){\cdot}CHCl_3\}_n$ (**5**) chains with $CHCl_3$ as solvent.

2. Experimental

2.1. *Physical measurements*

The C, H, and N analyses were carried out using a Leco 932-CHNS microanalyzer. Electronic spectra were recorded with a Shimadzu UV-265 FW spectrophotometer. Magnetic measurements were carried out from 5–300 K using a Quantum Design SQUID MPMSXL magnetometer with an applied field of 2000, 5000, and 10,000 G for complexes **1**, **3**, and **4**, respectively. Diamagnetic corrections were applied [26]. A correction for temperature independent paramagnetism (TIP) of $60 \times 10^{-6}\,cm^3\,mol^{-1}$ of Cu was applied in all cases. R for the data fitting was defined as $R = \Sigma[(\chi T)_{exp} - (\chi T)_{calc}]^2/\Sigma(\chi T)^2_{exp}$. Electron paramagnetic resonance (EPR) spectra were recorded on a Bruker ESP300 spectrometer with a Bruker ER 035 Gaussmeter and a HP 5325 frequency counter, in Q band, at room temperature, for powdered crystal (**1** and **3**) and powder (**4**).

2.2. *Synthesis*

2.2.1. [Cu_2(μ-AcO)$_4$(pydz)$_2$] (1). Pyridazine (0.18 mL, 2.4 mmol) was added to a solution of $Cu(AcO)_2 \cdot H_2O$ (199 mg, 1 mmol) in MeOH : $CHCl_3$ 1 : 1 (14 mL). The resulting green solution was stirred for 30 min at room temperature. After slow evaporation of the solvent, a green precipitate was formed. The solid was dissolved in acetonitrile (10 mL) and, by slow evaporation, crystals suitable for study by X-ray diffraction were formed. Yield: 219 mg, 84%. Anal. Calcd for $C_8H_{10}CuN_2O_4$ (%): C, 36.71; H, 3.85; and N, 10.70. Found (%): C, 36.40; H, 3.81; and N, 10.92.

2.2.2. {[Cu_2(μ-HCOO)$_4$](μ-pymd)}$_n$ (2). To a solution of $Cu(HCOO)_2 \cdot 4H_2O$ (226 mg, 1 mmol) in methanol (25 mL), pyrimidine (0.04 mL, 0.5 mmol) was added. The resulting solution was stirred for 5 h at room temperature. The green precipitate was filtered off, washed with methanol, and dried *in vacuo* over $CaCl_2$. Yield: 106 mg, 55%. Anal. Calcd for $C_4H_4CuNO_4$ (%): C, 24.81; H, 2.08; N, 7.23. Found (%): C, 24.41; H, 2.15; and N, 7.07. Crystals suitable for X-ray diffraction were obtained by slow evaporation of the reaction solution in the synthesis of the compound.

2.2.3. {[Cu_2(μ-AcO)$_4$](μ-pymd)}$_n$ (3). Pyrimidine (0.04 mL, 0.5 mmol) was added to a solution of $Cu(AcO)_2{\cdot}H_2O$ (200 mg, 1 mmol) in acetonitrile (25 mL). The resulting solution was stirred for 24 h at room temperature. The green precipitate was filtered off, washed with acetonitrile, and dried *in vacuo* over $CaCl_2$. Yield: 183 mg, 83%. Anal. Calcd for $C_6H_8CuNO_4$ (%): C, 32.51; H, 3.64; and N, 6.32. Found: C, 32.70; H, 3.57; and N, 6.41. Crystals suitable for X-ray diffraction were obtained by slow evaporation of a solution of the powder in methanol.

2.2.4. {[Cu_2(μ-AcO)$_4$](μ-4,4′-bipy)}$_n$ (4) and {[Cu_2(μ-AcO)$_4$](μ-4,4′-bipy)•$CHCl_3$}$_n$ (5). A solution of 4,4′-bipyridine (78 mg, 0.5 mmol) in acetonitrile (8 mL) was added to a solution of $Cu(AcO)_2{\cdot}H_2O$ (200 mg, 1 mmol) in acetonitrile (40 mL). The resulting solution was stirred for 90 min at room temperature. The green precipitate of **4** was filtered off, washed with acetonitrile, and dried *in vacuo* over $CaCl_2$. Yield: 219 mg, 84%. Anal. Calcd for $C_9H_{10}CuNO_4$ (%): C, 41.62; H, 3.88; and N, 5.39. Found (%): C, 41.29; H, 4.01; and N, 5.81. Crystals of **5**, suitable for X-ray diffraction, were obtained by a three capped disposition of 4,4′-bipy (156 mg, 1 mmol) in $CHCl_3$ (10 mL), CH_3OH : $CHCl_3$ and $Cu(AcO)_2{\cdot}H_2O$ (200 mg, 1 mmol) in CH_3OH (15 mL).

2.3. *X-ray crystallographic study*

Data collection was carried out at room temperature on a Bruker Smart CCD diffractometer using graphite-monochromated Mo-Kα radiation ($\lambda = 0.71073$ Å) operating at 50 kV and 25 mA. Data were collected over a hemisphere of the reciprocal space by combination of three exposure sets. Each exposure of 30 s (**1**) or 20 s (**2**, **3**, and **5**) covered 0.3 in ω. The cell parameter was determined and refined by a least-squares fit of all reflections. The first 50 (**1** and **5**), 100 (**2** and **3**) frames were collected at the end of the data collection to monitor crystal decay and no appreciable decay was observed.

A summary of the fundamental crystals and refinement data is given in table 1. No absorption correction was applied. The structures were solved by direct methods and refined by full-matrix least-square procedures on F^2 [27]. All non-hydrogen atoms were refined anisotropically. All hydrogens were included at their calculated positions determined by molecular geometry and refined riding on the corresponding carbons.

3. Results and discussion

3.1. *Synthesis and spectroscopic properties*

Crystals of **5** were only obtained when using $CHCl_3$ in the reaction of 4,4′-bipyridine and $Cu(AcO)_2 \cdot H_2O$. The $CHCl_3$ molecule stabilizes the crystal structure in $\{[Cu_2(\mu\text{-}AcO)_4](\mu\text{-}4,4'\text{-bipy}) \cdot CHCl_3\}_n$. In analogous compounds described in the literature [21–23] the crystal structure always contains a solvent of crystallization.

In the visible region of the diffuse reflectance spectra of the complexes the broad band assigned to the d–d transitions is observed to be centered at 690–725 nm, and the absorption at 380 nm, characteristic of the $[Cu_2(\mu\text{-}RCOO)_4]$ group, is observed.

3.2. *Description of the structures*

3.2.1. Crystal structure of $[Cu_2(\mu\text{-}AcO)_4(pydz)_2]$ (1). The crystal structure of **1** consists of centrosymmetric dimeric molecules with a molecule of pyridazine coordinated to each copper in the $[Cu_2(\mu\text{-}AcO)_4]$ unit (figure 1a). The pyridazine is monodentate due to the relative position of the two nitrogens. Selected interatomic distances and angles are collected in table 2. The trigonality index [28] deduced from the angles data, $\tau = 0.0036$, corresponds to a square pyramidal geometry. The bond distances are normal for square pyramidal coordination of copper. The Cu–N distance (2.211(3) Å) for the axial nitrogen is longer than the Cu–N distance (2.045(3) Å) for the equatorial nitrogen in the octahedral coordination of copper in $Cu(pydz)Cl_2$ [19].

The copper rises from the plane defined by O1O2O3O4 to N1 by 0.2118(4) Å. The two pyridazine rings of each dinuclear molecule are coplanar and almost parallel to the plane N1Cu1O1O3. The dimers have two different orientations in the crystal. Rows of dimers of the same orientation are observed along *b*- and *c*-axes and they form sheets parallel to *bc* plane (figure 1b).

3.2.2. Crystal structure of $\{[Cu_2(\mu\text{-}HCOO)_4](\mu\text{-}pymd)\}_n$ (2). The crystal structure of **2** consists of *zig-zag* chains of $[Cu_2(\mu\text{-}HCOO)_4]$ centrosymmetric units linked by pyrimidine molecules (figure 2a). The pyrimidine molecules are coordinated to two coppers in axial positions through nitrogens. The C3 and C5 atoms define a binary axis.

Table 1. Crystallographic and structure refinement data for **1–3** and **5**.

	1	**2**	**3**	**5**
Empirical formula	$C_{16}H_{20}Cu_2N_4O_8$	$C_8H_8Cu_2N_2O_8$	$C_{12}H_{16}Cu_2N_2O_8$	$C_{19}H_{21}Cu_2Cl_3N_2O_8$
Formula weight	523.44	387.24	443.35	638.81
Wavelength (Å)	0.71073	0.71073	0.71073	0.71073
Crystal system	Orthorhombic	Monoclinic	Triclinic	Monoclinic
Space group	*Pbca*	*C*2/*c*	$P\bar{1}$	*C*2/*c*
Unit cell dimensions				
a (Å)	12.996(1)	13.920(3)	8.241(1)	23.579(2)
b (Å)	8.640(7)	6.858(1)	9.361(1)	14.035(1)
c (Å)	19.233(2)	13.078(3)	10.965(2)	15.761(2)
α (°)	–	–	92.529(3)	–
β (°)	–	101.885(4)	97.745(3)	108.067(2)
γ (°)	–	–	102.845(3)	–
Volume (Å^3), *Z*	2159.7(3), 4	1221.7(4), 4	814.8(2), 2	4958.7(8), 8
Calculated density (g cm^{-3})	1.610	2.105	1.807	1.711
Absorption coefficient (mm^{-1})	2.018	3.522	2.653	2.085
F(000)	1064	768	448	2576
Scan technique	φ and ω	φ and ω	φ and ω	φ and ω
θ range for data collection (°)	2.12–28.93	2.99–28.79	1.88–26.37	1.71–28.98
Index ranges	(−16, −11, 23)–(17, 9, 25)	(−17, −9, −15)–(18, 9, 16)	(−10, −8, −11)–(10, 11, 13)	(−30, −18, −16)–(30, 18, 20)
Reflections collected	12,947	5177	6995	23,350
Independent reflections	2685 [*R*(int) = 0.0843]	1482 [*R*(int) = 0.0766]	3209 [*R*(int) = 0.0720]	6137 [*R*(int) = 0.0667]
Data/restraints/parameters	2685/0/138	1482/0/92	3209/0/221	6137/0/310
Goodness-of-fit on F^2	0.923	0.99	1.00	0.952
Final *R*(*) indices [$I > 2\sigma(I)$]	0.0386 (1566 obs.)	0.0363 (1055 obs.)	0.0367 (2239 obs.)	0.0403 (3641 obs.)
wR_2 (all data)	0.1012	0.0882	0.1118	0.1139
Largest difference peak and hole (e Å^{-3})	0.363 and −0.429	0.633 and −0.598	0.521 and −0.571	0.528 and −0.615

$R_1 = \Sigma||F_o| - |F_c||/\Sigma|F_o|$ and $wR_2 = [\Sigma w(F_o^2 - F_c^2)^2/\Sigma w(F_o^2)^2]^{1/2}$.

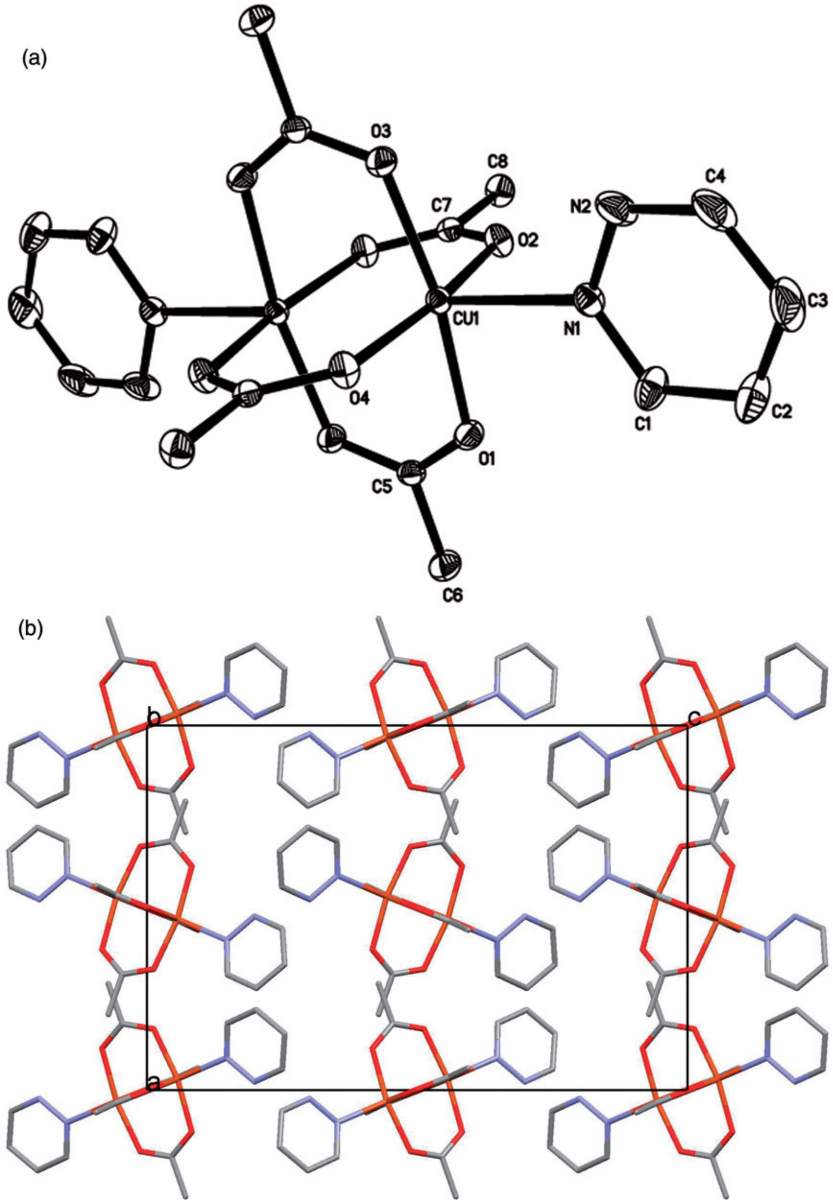

Figure 1. (a) ORTEP view of **1** showing the atomic numbering (30% probability ellipsoids). Hydrogens have been omitted for clarity. (b) Packing of the dimers of **1**. View along the *b*-axis.

Selected interatomic distances and angles are collected in table 2. The bond distances are the normal for this square pyramidal coordination of copper. The trigonality index [28], $\tau = 0.0015$, corresponds to square pyramidal geometry. The copper rises from the plane defined by O1O2O3O4 to N1 by 0.1933(4) Å. The chains run in the (1 0 1) direction in the crystal.

Table 2. Selected interatomic distances (Å) and angles (°) for **1** and **2**.

	1	**2**
Cu1–O1	1.975(2)	1.980(3)
Cu1–O2	1.972(2)	1.961(3)
Cu1–O3	1.959(2)	1.972(2)
Cu1–O4	1.964(2)	1.970(2)
Cu1–N1	2.211(3)	2.186(3)
Cu1 ··· Cu1A	2.6440(7)	2.6213(8)
Cu1 ··· Cu1B		6.1645(8)
O1–Cu1–O2	88.2(1)	88.0(1)
O1–Cu1–O3	167.7(1)	168.7(1)
O1–Cu1–O4	89.8(1)	90.5(1)
O2–Cu1–O3	89.8(1)	90.0(1)
O2–Cu1–O4	167.5(1)	168.8(1)
O3–Cu1–O4	89.5(1)	89.2(1)
N1–Cu1–O1	93.2(1)	94.1(1)
N1–Cu1–O2	96.5(1)	101.3(1)
N1–Cu1–O3	99.0(1)	97.2(1)
N1–Cu1–O4	95.9(1)	89.9(1)
N1–Cu1–Cu1A	176.9(1)	171.4(1)
Torsion angles		
O4–Cu1–N1–C1	81.3(3)	
O3–Cu1–N1–C1	171.8(3)	
O2–Cu1–N1–C1	−97.4(3)	
O1–Cu1–N1–C1	−8.8(3)	
O4–Cu1–N1–N2	−92.7(3)	
O3–Cu1–N1–N2	−2.2(3)	
O2–Cu1–N1–N2	88.5(3)	
O1–Cu1–N1–N2	177.1(2)	

Symmetry transformations: **1**: A, $-x$, $-y+1$, and $-z+2$; **2**: A, $-x+1/2$, $-y+1/2$, and $-z+1$; B, $-x+1$, y and $-z+3/2$.

3.2.3. Crystal structure of {[Cu$_2$(μ-AcO)$_4$](μ-pymd)}$_n$ (3). The asymmetric unit in the *zig-zag* chains of **3** consists of two independent coppers: Cu1 and Cu2 (figure 2b). Selected interatomic distances and angles are collected in table 3. The bond distances are normal for this square pyramidal coordination of copper. The trigonality index [28], $\tau = 0.0018$ (Cu1) and 0.0038 (Cu2), correspond to square pyramidal geometry. Cu1 rises from the plane defined by O1O2O3O4 to N1 by 0.1943(5) Å and Cu2 by 0.1921(5) Å to N2 from the plane defined by O5O6O7O8. The *zig-zag* chains run in the (1 1 −2) direction in the crystal (figure 2c).

3.2.4. Crystal structure of {[Cu$_2$(μ-AcO)$_4$](μ-4,4′-bipy)·CHCl$_3$}$_n$ (5). The crystal structure of **5** consists of chains of [Cu$_2$(μ-CH$_3$COO)$_4$] units linked by 4,4′-bipyridine (figure 3a). The 4,4′-bipyridine molecules are coordinated to two coppers in axial positions. There are chains of two types: I, with two independent coppers (Cu1 and Cu2), in which N1Cu1Cu2N2 define a binary axis, and II, with one independent Cu (Cu3), centrosymmetric in the dimer. In table 4 selected interatomic distances and angles are given. These data are usual for dinuclear units of copper. The trigonality index, $\tau = 0.126$ (Cu1), 0.122 (Cu2), and 0.0005 (Cu3), correspond to square pyramidal geometry, more distorted in the chain type I. The two pyridine rings coordinated to a

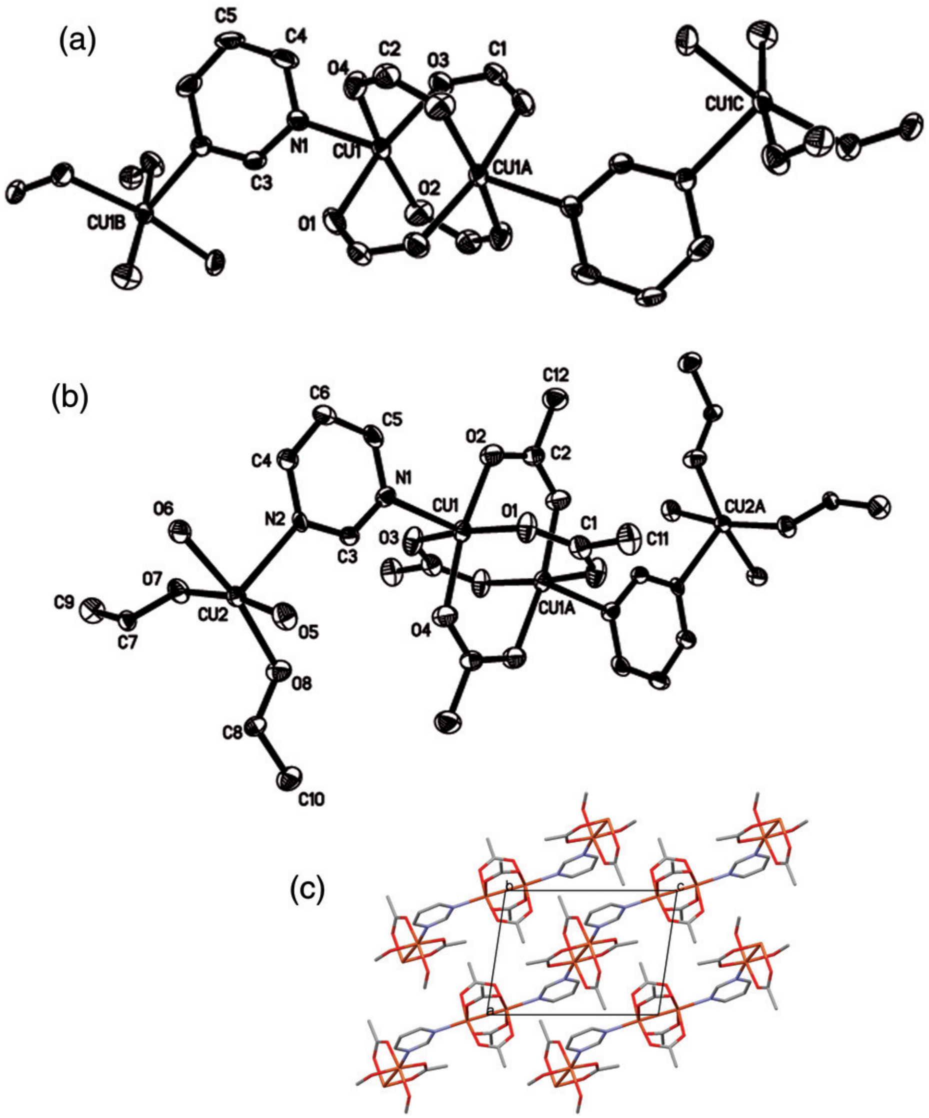

Figure 2. (a) ORTEP view of the asymmetric unit in the chain of **2** (30% probability ellipsoids). Hydrogens have been omitted for clarity. (b) ORTEP view of the asymmetric unit in the chain of **3** (20% probability ellipsoids). Hydrogens have been omitted for clarity. (c) Disposition of the chains in the crystal of **3**. View along the *b*-axis.

dimer (of a molecule of 4,4′-bipyridine) are coplanar in chain type II and form an angle of 57.1(2)° in chain type I.

The chains run parallel to the *b*-axis in the crystal (figure 3b). The $CHCl_3$ molecules are located in the interchain space with relatively short distances between Cl and O: 3.115(3) and 3.016(3) Å, shorter than the sum of the van der Waals radii of Cl and O (3.20 Å). Two chlorines of each $CHCl_3$ are close to two oxygens (O4 and O7) of two parallel chains (figure 3c). Each chain I dimer is in close contact (through O4 and O4A)

Table 3. Selected interatomic distances (Å) and angles (°) for **3**.

Cu1–O1	1.964(3)	Cu2–O5	1.978(3)
Cu1–O2	1.978(3)	Cu2–O6	1.971(3)
Cu1–O3	1.967(3)	Cu2–O7	1.996(3)
Cu1–O4	1.978(3)	Cu2–O8	1.969(3)
Cu1–N1	2.222(3)	Cu2–N2	2.203(3)
Cu1 ··· Cu1A	2.612(1)	Cu2 ··· Cu2B	2.607(1)
Cu1 ··· Cu2	6.108(1)		
O1–Cu1–O2	97.9(2)	O5–Cu2–O6	89.1(1)
O1–Cu1–O3	168.7(1)	O5–Cu2–O7	168.7(1)
O1–Cu1–O4	90.2(2)	O5–Cu2–O8	88.9(1)
O2–Cu1–O3	90.8(2)	O6–Cu2–O7	90.4(1)
O2–Cu1–O4	168.6(1)	O6–Cu2–O8	168.9(1)
O3–Cu1–O4	88.8(2)	O7–Cu2–O8	89.5(1)
N1–Cu1–O1	97.1(1)	N2–Cu2–O5	99.1(1)
N1–Cu1–O2	99.3(1)	N2–Cu2–O6	92.6(1)
N1–Cu1–O3	94.1(1)	N2–Cu2–O7	92.2(1)
N1–Cu1–O4	92.0(1)	N2–Cu2–O8	98.5(1)
N1–Cu1–Cu1A	173.5(1)	N2–Cu2–Cu2B	173.9(1)

Symmetry transformations used to generate equivalent atoms: A, $-x$, $-y+1$, and $-z+2$; B, $-x+1$, $-y+2$, and $-z+1$.

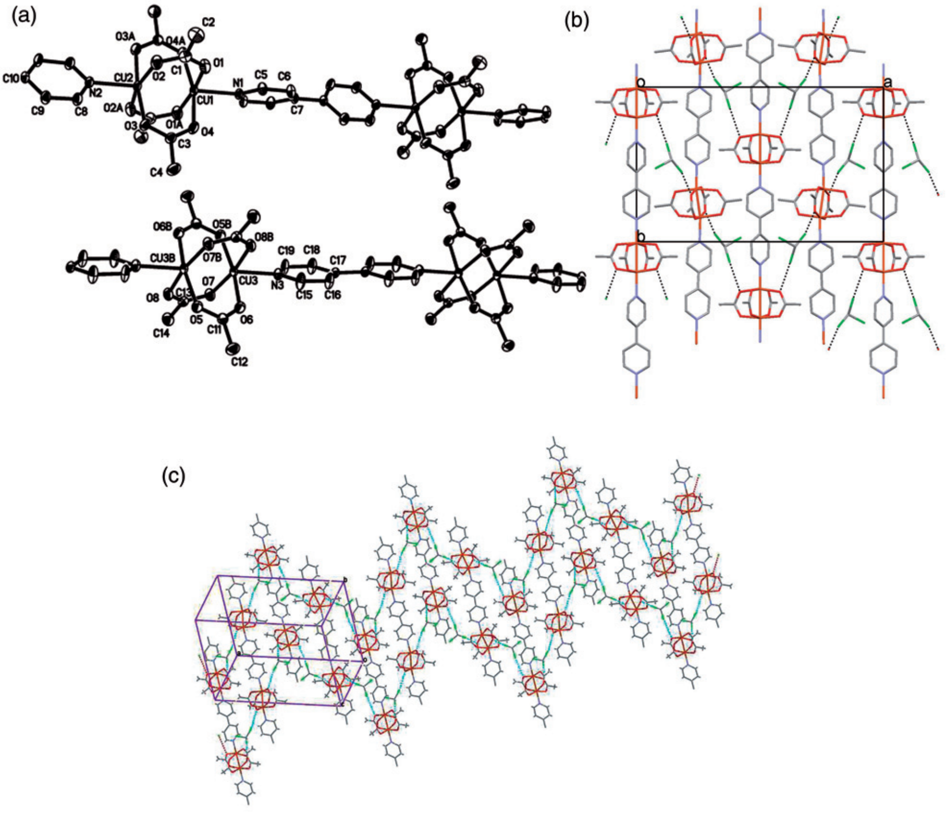

Figure 3. (a) ORTEP view of the chains in **5** showing the atomic numbering (30% probability ellipsoids). Hydrogens have been omitted for clarity. (b) View of **5** along *c*. (c) Disposition of the chains in the crystal of **5**.

Table 4. Selected interatomic distances (Å) and angles (°) for **5**.

Cu1–O1	1.961(3)	Cu2–O2	1.990(3)	Cu3–O6	1.970(2)
Cu1–O4	1.998(2)	Cu2–O3	1.951(2)	Cu3–O7	1.965(2)
Cu1–N1	2.180(3)	Cu2–N2	2.161(4)	Cu3–O8B	1.986(2)
Cu1 ··· Cu2	2.6311(8)			Cu3–O5B	1.980(2)
				Cu3–N3	2.202(3)
				Cu3 ··· Cu3B	2.6319(8)
O1–Cu1–O4	89.4(1)	O2–Cu2–O3	89.9(1)	O6–Cu3–O7	90.2(1)
O1–Cu1–O1A	171.4(1)	O2–Cu2–O2A	164.5(1)	O6–Cu3–O5B	168.3(1)
O1–Cu1–O4	89.4(1)	O2–Cu2–O3A	89.1(1)	O6–Cu3–O8B	89.7(1)
O4–Cu1–O4A	163.8(1)	O3–Cu2–O3A	171.8(1)	O7–Cu3–O5B	89.2(1)
N1–Cu1–O1	94.3(1)	N2–Cu2–O2	97.8(1)	O7–Cu3–O8B	168.2(1)
N1–Cu1–O4	98.1(1)	N2–Cu2–O3	94.1(1)	O5B–Cu3–O8B	88.7(1)
				N3–Cu3–O6	92.4(1)
				N3–Cu3–O7	103.7(1)
				N3–Cu3–O5B	99.2(1)
				N3–Cu3–O8B	88.1(1)
				N3–Cu3–Cu3B	168.6(1)
Cl(1)–C(20)	1.769(4)	Cl(1) ··· O(4)	3.115(3)		
Cl(2)–C(20)	1.743(4)	Cl(2) ··· O(7)	3.016(3)		
Cl(3)–C(20)	1.735(4)				

Symmetry transformations used to generate equivalent atoms: A, $-x+1$, y, and $-z+1/2$; B, $-x+1/2$, $-y+3/2$, and $-z$.

with two dimers (through O7) of two chains type II and each dimer of chain type II is in close contact (through O7 and O7B) with two dimers (through O4) of two chains type I. In this way, the packing can be described as sheets parallel to the (1 0 −1) plane (figure 3c).

In $Cu_2(AcO)_4$(4,4′-bipy) · DMF, there is only one type of chain, with the two rings of each 4,4′-bipy molecule approximately coplanar. The crystal structure is described as 2-D layers constructed by intermolecular π–π interactions of the bipy rings from adjacent 1-D chains [23, 24]. For **4**, without solvent molecule, the presence of 1-D chains is proposed.

3.3. *Magnetic and EPR results*

Compounds **1**, **3**, and **4** show strong antiferromagnetism. The magnetic moments decrease from 1.63, 1.55, and 1.26 μ_B at 300 K to 0.20, 0.09, and 0.27 μ_B at 5 K, for **1**, **3**, and **4**, respectively.

The χT experimental data, from 5 to 300 K, were fitted to the Bleaney–Bowers equation for a dimer with $S_1 = S_2 = 1/2$, modified by the inclusion of the fraction of monomeric impurity [29]:

$$\chi_M(2\mathrm{Cu}) = [C2e^{2x}(1-\rho)/(1+3e^{2x})] + C\rho/2 + N\alpha$$

where $C = Ng^2\beta^2/kT$, $x = 2J/kT$, $2J$ = separation between singlet and triplet states, ρ is the fraction of monomeric impurity, and $N\alpha$ is the TIP. The results for the best fit are collected in table 5. Figure 4 shows the plot of $\chi_M T$, per mole of dimer, *versus* temperature (T) for **3**. The possible interaction between coppers through the nitrogen ligand in **3** and **4** is considered negligible beside the strong antiferromagnetic effect of the *paddle-wheel* group [30].

Table 5. Magnetic results for **1**, **3**, and **4**.

Compound	μ_B (300 K)	μ_B (5 K)	g	$2J$ (cm^{-1})	ρ	R[a]
1	1.63	0.20	2.25	−226	0.017	1.1×10^{-3}
3	1.55	0.09	2.21	−298	0.011	3.3×10^{-3}
4	1.26	0.27	2.05	−340	0.028	3.4×10^{-4}

[a] $R = \Sigma[(\chi T)_{\text{exp}} - (\chi T)_{\text{calc}}]^2 / \Sigma(\chi T)^2_{\text{exp}}$.

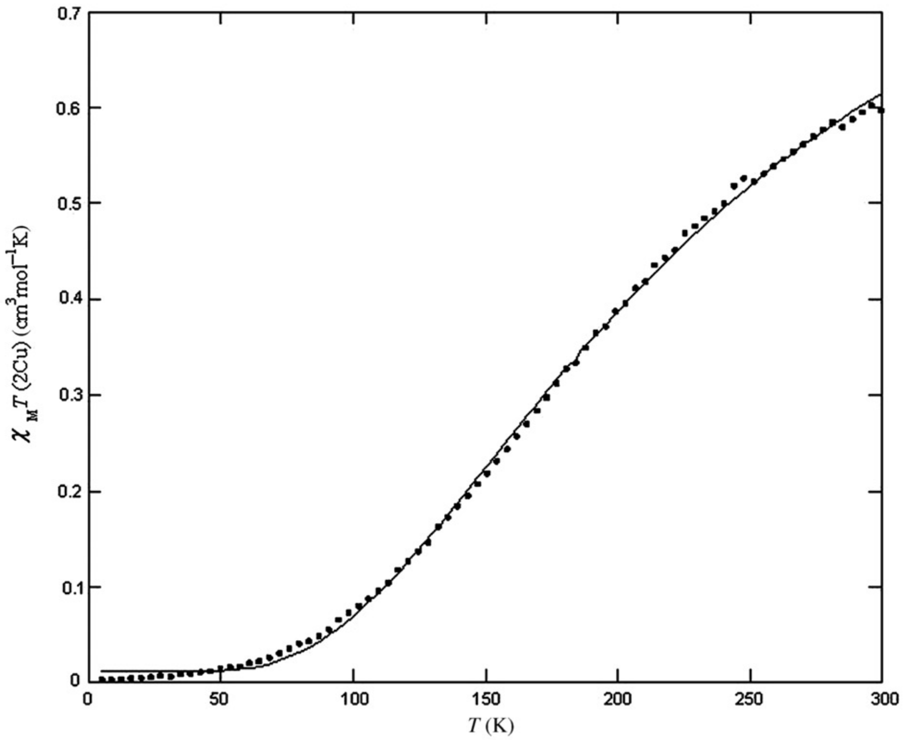

Figure 4. Plot of $X_M T$ *vs.* T, per mole of dimer for **3**.

The powder EPR spectra of **1**, **3**, and **4** at Q band and room temperature show signals of the triplet state ($S = 1$) for $D \neq 0$ and $E \approx 0$. Figure 5 corresponds to the spectrum of **1**. The spectra were interpreted according to the Wasserman, Snyder, and Yager equations [31] based on the Hamiltonian $H = gHS\beta + D[S_z^2 - 2/3] + E[S_x^2 - S_y^2]$, with $D \neq 0$ and $E = 0$.

For $\Delta M = \pm 1$:

$$H_{\parallel} = (g_e/g_{\parallel})(H_o - D')$$
$$H_{\perp 1} = (g_e/g_{\perp})[H_o(H_o - D')]^{1/2}$$
$$H_{\perp 2} = (g_e/g_{\perp})[H_o(H_o + D')]^{1/2}$$

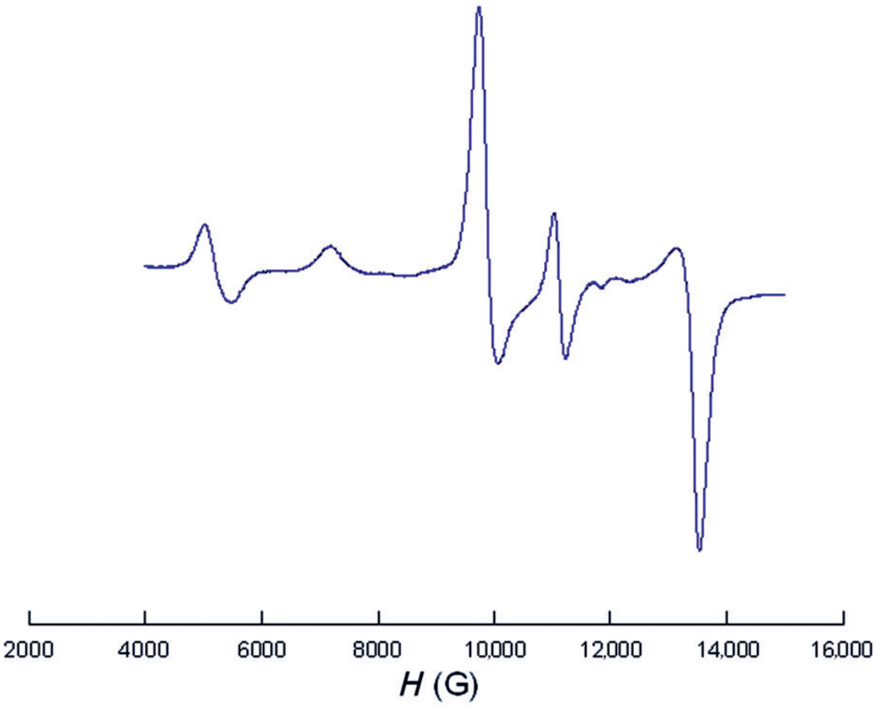

Figure 5. EPR Q band ($\nu = 34.0846$ GHz) spectrum of powered crystal of **1** at room temperature.

Table 6. EPR results for **1**, **3**, and **4**.

Compound	$H_{\min}$ (G)	$H_{\parallel}$ (G)	$H_{\perp 1}$ (G)	$H_{\perp 2}$ (G)	H_{dq} (G)	$g_{\parallel}$	$g_{\perp}$	g_{av}	D (cm^{-1})
1	4900	7158	9738	13,532	11,115	2.32	2.07	2.15	0.361
3			9758	13,502	11,134	2.30	2.06	2.15	0.36
4	4999	7138	9708	13,472	11,067	2.33	2.07	2.16	0.359

For $\Delta M = \pm 2$:

$$H_{\min} = (g_e/g_{\min})[(H_o^2/4) - (D'^2/3)]^{1/2}$$
$$H_{dq} = (g_e/g_{av})[H_o^2 - D'^2/3]^{1/2}$$
$$H_o = h\nu/g_e\beta;\ D' = D/g_e\beta$$

The experimental values of H and the calculated parameters: $g_{\parallel}$, $g_{\perp}$, g_{av}, and D are collected in table 6. The $2J$ and D values are similar for other *paddle-wheel* systems of acetate [13, 14].

4. Conclusions

We describe acetate and formate complexes formed by $[Cu_2(\mu\text{-RCOO})_4]$ *paddle-wheel* units and dinitrogen ligands coordinated to the apical positions of copper. Depending on the relative position of nitrogens in the ligand, different results are obtained. The pyridazine, with two nitrogens in 1,2 positions is monodentate giving **1**. Pyrimidine, with nitrogens in 1,3 positions, is bidentate giving *zig-zag* chains in **2** and **3**. For the formate compound (**2**), the dimeric unit is centrosymmetric and for the acetate (**3**), there are two independent Cu atoms.

In **5**, the crystal structure, formed by monodimensional chains of $\{[Cu_2(\mu\text{-AcO})_4](\mu\text{-}4,4'\text{-bipy})\}_n$, is stabilized by $CHCl_3$.

Magnetic and EPR results are consistent with the presence of dimeric antiferromagnetic *paddle-wheel* copper(II) units.

Supplementary material

CCDC-733257, -733258, -733259, and -733260 for **1**, **2**, **3**, and **5**, respectively, contain the supplementary crystallographic data for this study. These data can be obtained free of charge from the Cambridge Crystallographic Data Centre *via* www.ccdc.cam.ac.uk/data_request/cif.

Acknowledgment

This study was supported by the "Diputación Foral de Gipuzkoa" in a programme cofinanced by the European Union (FEDER).

References

[1] P. De Mester, S.R. Fletcher, A.C. Skapski. *J. Chem. Soc., Dalton Trans.*, 2575 (1973).
[2] R.L. Carlin. *Magnetochemistry*, p. 77, Springer, Berlin-Heidelberg (1986).
[3] J. Catterick, P. Thornton. In *Advances in Inorganic Chemistry and Radiochemistry*, H.J. Emeleus, A.G. Sharpe (Eds), Vol. 20, p. 291, Academic Press, New York, London (1977).
[4] R.J. Doednes. In *Progress in Inorganic Chemistry*, Stephen J. Lippard (Ed.), Vol. 21, p. 209, John Wiley and Sons, New York (1976).
[5] V.M. Rao, D.N. Sathyanarayana, H. Manohar. *J. Chem. Soc., Dalton Trans.*, 2167 (1983).
[6] M. Nakagawa, Y. Inomata, F.S. Howell. *Inorg. Chim. Acta*, **295**, 121 (1999).
[7] D.B.W. Yawney, R.J. Doedens. *Inorg. Chem.*, **9**, 1626 (1970).
[8] F. Sapiña, M. Burgos, E. Escriva, J.V. Folgado, P. Gómez Romero. *Inorg. Chim. Acta*, **216**, 185 (1994).
[9] R. Cejudo, G. Alzuet, J. Borrás, M. Liu-González, F. Sanz-Ruiz. *Polyhedron*, **21**, 1057 (2002).
[10] M. Bukowska-Strzyzewska. *Rocz Chem.*, **40**, 567 (1966).
[11] M. Barquín, M.J. González Garmendia, L. Larrínaga, E. Pinilla, M.R. Torres. *Z. Anorg. Allg. Chem.*, **631**, 2210 (2005).
[12] R. Kiriyama, H. Ibamoto, K. Matsuo. *Acta Crystallogr.*, **7**, 482 (1954).
[13] J.M. Seco, M.J. González Garmendia, E. Pinilla, M.R. Torres. *Polyhedron*, **21**, 457 (2002).
[14] M. Barquín, M.J. González Garmendia, S. Pacheco, E. Pinilla, S. Quintela, J.M. Seco, M.R. Torres. *Inorg. Chim. Acta*, **35**, 3230 (2004).
[15] M. Barquín, M.J. González Garmendia, S. Pacheco, L. Larrínaga, E. Pinilla, M.R. Torres. *Inorg. Chim. Acta*, **359**, 2424 (2006).
[16] R. Sarma, J.B. Baruah. *J. Coord. Chem.*, **61**, 3329 (2008).
[17] M.J. González Garmendia, V. San Nancianceno, J.M. Seco, F.J. Zúñiga. *Acta Cryst.*, **C65**, m436 (2009).
[18] D. Hagrman, C. Sangregorio, Ch.J. O'Connor, J. Zubieta. *J. Chem. Soc., Dalton Trans.*, 3707 (1998).
[19] Th. Fetzer, A. Lentz, T. Debaerdemaeker, O. Abou-El-Wafa. *Z. Naturforsch.*, **45b**, 199 (1990).

[20] S.A. Barnett, N.R. Champness, C. Wilson. *Eur. J. Inorg. Chem.*, 1572 (2005).

[21] J.L. Manson, J. Gu, J.A. Schlueter, H.H. Wang. *Inorg. Chem.*, **42**, 3950 (2003).

[22] J.L. Manson, J.G. Lecher, J. Gu, U. Geiser, J.A. Schlueter, R. Henning, X. Wang, A.J. Schultz, H.J. Koo, M.H. Wangbo. *J. Chem. Soc., Dalton Trans.*, 2905 (2005).

[23] H.Y. Bie, J.H. Yu, K. Zhao, J. Lu, L.M. Duan, J.Q. Xu. *J. Mol. Struct.*, **741**, 77 (2005).

[24] S.W. Ng. *J. Mol. Struct.*, **791**, 201 (2006).

[25] Y.H. Wen, Y.H. He, Y.L. Feng, S.W. Ng. *Jiegou Huaxue (Chin. J. Struct. Chem.)*, **26**, 29 (2007).

[26] C.J. O'Connor. In *Progress in Inorganic Chemistry*, Stephen J. Lippard (Ed.), Vol. 29, p. 209, John Wiley and Sons, New York (1982).

[27] G.M. Sheldrick, *SHELX97, Program for Refinement of Crystal Structure*, University of Göttingen, Göttingen, Germany (1997).

[28] A.W. Addison, T.N. Rao, J. Reedjik, J. Van Rijn, G.C. Verschoor. *J. Chem. Soc., Dalton Trans.*, 1349 (1984).

[29] C.J. O'Connor. In *Progress in Inorganic Chemistry*, Stephen J. Lippard (Ed.), Vol. 29, p. 239, John Wiley and Sons, New York (1982).

[30] H. Hou, L. Xie, G. Li, T. Ge, Y. Fan, Y. Zhu. *New J. Chem.*, **28**, 191 (2004).

[31] A. Bencini, D. Gatteschi. *EPR of Exchange Coupled Systems*, p. 174, Springer, Berlin (1990).